Journal of
Mechanical
Science and
Technology

Journal of Mechanical Science and Technology 21 (2007) 2196~2204

Computational fluid dynamics analysis of greenhouse microclimates by heated underground tubes

Abel Rouboa[1,*] and Eliseu Monteiro[2]

[1]*CITAB-UTAD/Department of Mechanical Engineering and Applied Science, University of Pennsylvania, Philadelphia, PA 19104-6391*

[2]*Engineering Department of University of Trás-os-Montes e Alto Douro 5000, Vila Real, Portugal.*

(Manuscript Received June 22, 2006; Revised August 16, 2007; Accepted September 30, 2007)

Abstract

One of the main problems of Mediterranean climates is the large diurnal amplitude of temperature, with too low temperature during winter nights and too high temperatures during summer days. This is particularly felt in the north of Portugal, where the low temperature during winter nights can be compensated by the introduction of a heat source. The objective of this is work is to simulate the effects in the temperature and velocity fields by the introduction of hot water tubes along a greenhouse in night conditions. Three different situations are simulated: natural convective heating (case A), artificial heating tubes (case B), artificial heating tubes, and natural ventilation (case C). The commercial CFD package ANSYS® (FLOTRAN module) is used for this propose. The turbulence is modelled by the RNG turbulence model. The numerical results are compared with experimental values, the procedure for which is also presented.

The average increase in air temperature for cases A, B and C was 2.2°C, 6.7°C and 3.5°C, respectively. Turbulence is lower in case A, increases slightly when the heating system is introduced (case B), and increases significantly in case C due to the effect of natural ventilation. A very good agreement between experimental and numerical temperature values was verified. This allows validating the RNG turbulence model as suitable to simulate arch-shaped greenhouse microclimates. Some improvements can be done to this work: introduction of night-time crop transpiration, 3D simulations, or optimizing the size of the element mesh in order to reduce the computation time.

Keywords: Greenhouses; Artificial heating tubes; CFD; Finite element method

1. Introduction

Greenhouses commonly used in Southern European countries are multi-span structures with arch-shaped roofs covered by a plastic film. These Mediterranean greenhouses are equipped with roof or side vents, or both roof and side vents. The vents generally are continuous and the number of spans is normally small to increase ventilation through the side vent opening.

One of the main problems of Mediterranean climates is the large diurnal amplitude of air and soil temperature, with too low temperatures during winter nights and too high temperatures during summer days. This work is focuses on the problem of low temperatures during winter nights in Mediterranean climates, particularly in the north of Portugal. The introduction of heat sources in confined spaces induces the temperature to increase. This temperature increase also induces natural convection inside the confined space.

Natural ventilation is considered one of the most important factors of a greenhouse environment, since it directly affects transport of sensible, latent heat and CO_2 concentration to or from the interior air. In the Mediterranean area efficient climatization is crucial in order to decrease the inside air temperature and to remove excess humidity [1].

*Corresponding author. Tel.: +1 215 898 7998, Fax.: +1 215 573 6334
E-mail address: rouboa@seas.upenn.edu

The objective of this is work was to simulate the effects of temperature and velocity fields inside a greenhouse by the introduction of hot water tubes along the greenhouse. This was done by using the CFD technique, due to its advanced stage of development and its increasing utilization in various horticultural and agricultural studies [2].

The first CFD simulations were carried out by Okushima et al. [3], who compared their numerical results with the wind tunnel results of Sase et al. [4]. Even though their results agreed weakly, due to model limitations to accurately describe the grid, they obtained important information on flow patterns inside the greenhouse.

Mistriotis et al. [5,6] performed simulations with a 2D greenhouse model by applying the standard k-ε, the two-layer k-ε and the RNG models. They showed that all these models described the flow pattern correctly, but the standard k-ε model did not clearly reveal the reverse flow at the leeward roof. The same authors [7] performed 3D simulations with a twin-span Mediterranean greenhouse applying the Chen-Kim (CK) turbulence model [8]. The predictions of the average flow velocity in the vent opening, an outflow in the front of the vent opening changing to inflow at the end, showed a clear quantitative agreement with experimental data.

Boulard et al. [9] analyzed the buoyancy-driven flow in a closed greenhouse. Predictions of the internal flow, turbulent kinetic energy distribution and temperature distribution were made and compared with experimental data. Despite good qualitative agreement, quantitative differences were found for all variables. A similar approach for buoyancy-driven natural ventilation was suggested, which the subject of the work was presented in Boulard et al. [10] and Haxaire et al. [11,12] . The three papers essentially present the same results. Both single side and double sided ventilation, driven by buoyancy forces, were studied and airflow and temperature distributions were simulated. There was good agreement between measurements and simulated values, but details of the predictions, near the vent openings in particular, were different. This can be explained due to the application of the standard k-ε turbulence model instead of the more suitable RNG or CK model for separating flow, which occurs near the openings, as suggested by Mistriotis et al. [7].

It is clear that the RNG or CK turbulence models are the most suitable to simulate the greenhouse microclimate. In this work we use the RNG turbulence model available in the *FLOTRAN* module of *ANSYS*® to simulate the indoor air temperature and velocity fields in a polyethylene greenhouse in the north of Portugal, in night conditions, and for three different cases:

Case A: natural convective heating (no heating system and no natural ventilation effect);

Case B: AHT - artificial heating tubes (with heating system and no natural ventilation effect);

Case C: AHT and natural ventilation (heating system and natural ventilation effect).

The numerical results are compared with experimental values, this procedure is also presented. The distinctive aspects of this work are the analysis of the effects of heating tubes in Mediterranean greenhouse indoor air characteristics during the night and the use of the finite element method instead of the finite volume method usually applied in a CFD simulation. This analysis could lead to further improvement in the design of Mediterranean greenhouse heating systems in order to improve the climate control during winter nights.

2. Materials and methods

2.1 Experimental set up

Experiments were carried out in a 22 m length, 8.5 m width and 3.5 m height greenhouse with polyethylene cover and vent openings. A schematic view of the experimental greenhouse is shown in Fig 1.

The greenhouse is located in the north of Portugal, and since this region is characterized by a predominant northerly wind, symmetric airflow was assumed along the direction of each opening. Therefore, a cross section was selected to explore the flow patterns. The outdoor air velocity and temperature were meas-

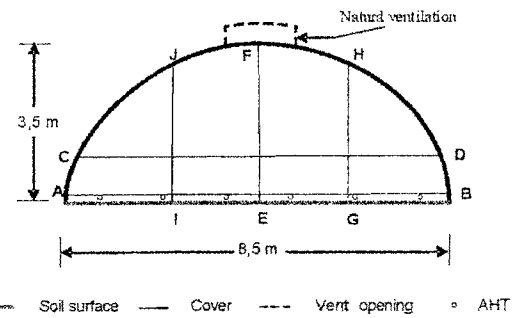

Fig. 1. Schematic Design of the Experimental Greenhouse.

Table 1. Co-ordinates of the nodes used in the analyzed paths.

Co	A	B	C	D	E	F	G	H	I	J
X	0.01	8.49	0.50	8.00	4.25	4.25	6.20	6.20	2.30	2.30
Y	0.125	0.125	1.00	1.00	0.00	3.50	0.00	3.10	0.00	3.10

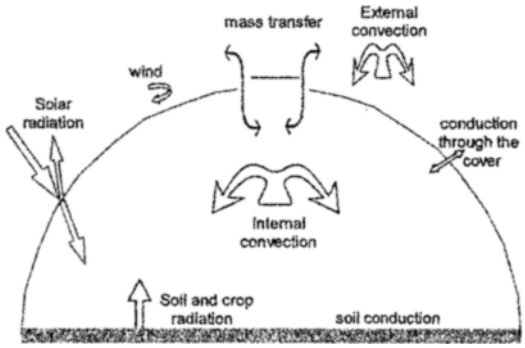

Fig. 2. Heat and mass transfer in greenhouses.

ured by two sonic anemometers.

In this region, it is during the night that the energy losses are important and can be compensated with an artificial heat input. On the other hand, in this type of climate, the energetic contribution from solar radiation usually avoids artificial heating needs during the day. During sunny days, the greenhouse usually needs to be ventilated because of the high level of temperature.

Fourteen K-type thermocouples were placed along the path CD (one meter from the soil) in order to measure the temperature. The coordinates of the nodes for the five paths represented in the Fig.1 are shown in Table 1.

2.2 Thermal modeling

Temperature, humidity, CO_2, solar radiation air velocity determines the greenhouse microclimate. These variables are affected by the external weather, by the properties of the greenhouse cover, and by the properties of the crops. Temperature and moisture relations within the soil-plant-atmosphere system determine the rates at which processes progress in the plant [13].

Several studies on analysis and control of the indoor greenhouse environment are based on the concept of heat, mass balance, and physical modeling. Fig. 1 shows the energy balance between the greenhouse and the environment.

The heat transfer between the greenhouse and the environment is complex, because it occurs by several ways:

By thermal radiation, from the soil, atmosphere, greenhouse environment and vegetation, emitted through greenhouse structure and cover;

Natural convection of the indoor air;

Forced convection caused by wind flow;

By conduction between soil surface and interior layer, and between cover walls.

The energy balance model used to represent a greenhouse climate is described by [14]. The rate of external heat required to maintain the temperature inside greenhouse is:

$$q = q_{sen} + q_{lat} + q_c + q_{sto} - q_{rad} \tag{1}$$

where q_{sen} are the sensible heat losses, q_{lat} the latent heat losses, q_c the conductive heat losses through the cover, q_{sto} the heat stored in greenhouse and q_{rad} the heat energy absorbed by the greenhouse.

The energy balance equation for a ventilated greenhouse is described by Bailey and Day [15] as follows.

$$A_c U(T_0 - T_g) + c_{air}\dot{V}\rho_{air}(T_0 - T_g) + \eta S = 0 \tag{2}$$

The energy losses through the cover (first three terms of equation (1)) are represented by the first term of equation (2), where the global heat transfer coefficient (U) is calculated as a linear function of the wind speed as follows:

$$U = a_0 + a_1 w \tag{3}$$

where a_0 and a_1 are empirical constants assuming, respectively, the values 4.0 W $m^{-2}K^{-1}$ and 1.0 W $m^{-3}s$ K^{-1} and w is the wind speed. The second term of equation (2) represents the ventilation energy losses. Terms q_{rad} and ηS of equation (1) and (2), respectively, represent the part of incident solar radiation that contributes to sensible heat gain of the greenhouse.

As far as physical models are concerned, the model described by Tap et al. [16] is extended to take into account the heating tube system. This improvement results in a set of three-coupled first order differential equations. The greenhouse temperature T_g is modeled by a first order equation with a constant greenhouse heat capacity c_g, and with heat flux from ventilation, cover, heating tubes, soil and sun.

$$\frac{dT_g}{dt}=\frac{1}{c_g}\left[(K_v+K_r)(T_e-T_g)+K_p(T_p-T_g)+K_s(T_s-T_g)+\eta_i S\right] \tag{4}$$

$$\frac{dT_s}{dt}=\frac{1}{c_s}\left[K_s(T_g-T_s)+K_d(T_d-T_s)\right] \tag{5}$$

$$\frac{dT_p}{dt}=\frac{1}{c_p}\left[K_p(T_g-T_p)+K_h(T_h-T_p)\right] \tag{6}$$

The main drawback of the models based on balance equations is that they do not provide details of internal flow patterns and temperature profiles. Recent progress in flow modelling by means of computational fluid dynamics (CFD) software facilitates the analysis of such scalar and vector fields by numerically solving transport equations, which are presented in the next section.

2.3 Mathematical model

The process of Reynolds-averaging the Navier-Stokes and scalar transport equations introduces additional terms containing correlations of the fluctuating velocity components, which must themselves be modelled in order to affect closure. A large number of models have been proposed, many based on the Boussinesq assumption, which relates the Reynolds stresses to the mean velocity gradient via a turbulent viscosity. The Boussinesq based two equation models have demonstrated a good balance between accuracy and efficiency. In particular, the k-ε turbulence model of Launder and Spalding [17] has been widely adopted, where transport equations are solved for the turbulent kinetic energy (k), and the rate of dissipation of the turbulent kinetic energy (ε). Various authors have proposed and tested modifications of the standard k-ε turbulence model. For instance, Costa et al. [18] compare eight versions of the k-ε turbulence model in internal convection flows. The conclusion was that the performance of the turbulence model is problem dependent, which means we cannot extrapolate results from different systems or geometries.

The finite volume method is a well-established CFD technique that is used in several commercial CFD codes such as FLUENT, PHOENICS, FLOW3D and STAR-CD. Recent developments of this technique were made in Kim and Choi [19], in Kim et al. [20] and Monteiro et al. [21] using, respectively, curvilinear formulation and parallel computation.

In this paper we use the FLOTRAN module of ANSYS®, which is finite element based. This simulation tool has six turbulence models available: Standard k-ε Model, Zero Equation Turbulence Model, Re-Normalized Group Turbulence Model (RNG), k-ε Model of Shih (NKE), Non-linear Model of Girimaji (GIR), Shih, Zhu, and Lumley Model (SZL). The mathematical model used in this work is composed of the continuity equation, energy conservation equation, momentum conservation equations and RNG turbulence model equations [22,23]. Steady-state regime and incompressible fluid are considered.

$$\frac{\partial(\rho V_x)}{\partial x}+\frac{\partial(\rho V_y)}{\partial y}=0 \tag{7}$$

$$\frac{\partial(\rho V_x V_x)}{\partial x}+\frac{\partial(\rho V_y V_x)}{\partial y}=\rho g_x-\frac{\partial P}{\partial x}+\frac{\partial}{\partial x}\left(\mu_e\frac{\partial V_x}{\partial x}\right)+\frac{\partial}{\partial y}\left(\mu_e\frac{\partial V_x}{\partial y}\right) \tag{8}$$

$$\frac{\partial(\rho V_x V_y)}{\partial x}+\frac{\partial(\rho V_y V_y)}{\partial y}=\rho g_y-\frac{\partial P}{\partial y}+\frac{\partial}{\partial x}\left(\mu_e\frac{\partial V_y}{\partial x}\right)+\frac{\partial}{\partial y}\left(\mu_e\frac{\partial V_y}{\partial y}\right) \tag{9}$$

$$\frac{\partial}{\partial x}\left(\rho V_x C_p T\right)+\frac{\partial}{\partial y}\left(\rho V_y C_p T\right)=\frac{\partial}{\partial x}\left(K\frac{\partial T}{\partial x}\right)+\frac{\partial}{\partial y}\left(K\frac{\partial T}{\partial y}\right) \tag{10}$$

$$\frac{\partial(\rho V_x \varepsilon)}{\partial x}+\frac{\partial(\rho V_y \varepsilon)}{\partial y}=\frac{\partial}{\partial x}\left(\frac{\mu_t}{\sigma_\varepsilon}\frac{\partial \varepsilon}{\partial x}\right)+\frac{\partial}{\partial y}\left(\frac{\mu_t}{\sigma_\varepsilon}\frac{\partial \varepsilon}{\partial y}\right)+C_{1\varepsilon}\mu_t\frac{\varepsilon}{k}\Phi-C_2\rho\frac{\varepsilon^2}{k}+\frac{C_\mu(1-C_3)\beta\rho k}{\sigma_t}\left(g_x\frac{\partial T}{\partial x}+g_y\frac{\partial T}{\partial y}\right) \tag{11}$$

Table 2. RNG turbulence model constants.

Constant	Value
C_1	1.44
C_2	1.68
C_3	1.0
C_4	0.0
C_ε	1.44
C_μ	0.085
σ_k	0.72
σ_ε	0.72
σ_t	1.0
β	0.12
λ	4.38

$$\frac{\partial(\rho V_x k)}{\partial x}+\frac{\partial(\rho V_y k)}{\partial y}=\frac{\partial}{\partial x}\left(\frac{\mu_t}{\sigma_\varepsilon}\frac{\partial k}{\partial x}\right)+\frac{\partial}{\partial y}\left(\frac{\mu_t}{\sigma_\varepsilon}\frac{\partial k}{\partial y}\right)+\mu_t\Phi-\rho\varepsilon+\frac{C_4\beta\mu_t}{\sigma_t}\left(g_x\frac{\partial T}{\partial x}+g_y\frac{\partial T}{\partial y}\right) \quad (12)$$

$$C_{1\varepsilon}=1.42-\frac{\lambda\left(1-\frac{\lambda}{\lambda_\infty}\right)}{1+\beta\lambda^3} \quad (13)$$

The values of the constants used in RNG turbulence model are presented in Table 2.

2.4 Solution method

The steady solution of the governing equations is given in each square element of the discretized whole domain. In order to solve the linear system, TDMA (Tri-Diagonal Matrix Algorithm) is used as the solver [24]. The convergence criterion of the TDMA solver is 10^{-5} for the two velocities components, V_x and V_y, and 10^{-3} for pressure, turbulence kinetic and turbulence energy dissipation ratio.

The requirements of meshes for turbulence model are more restrictive than those for laminar flow. Therefore, the "quad" element size has to be about 0.025 m, (Fig. 2). In the zone of high gradients of temperature, velocity or pressure, in particular near the walls, the mesh size was refined by a factor of four.

Fig. 3. Element mesh of the 2D model of the greenhouse.

Table 3. Boundary conditions.

	Gravity (m/s^2)	Temperature (°C)				Exterior air velocity (m/s)
		Floor	Cover	Heater	Exterior air	
A	9.81	10	-3	-	-	-
B	9.81	10	-3	60	-	-
C	9.81	10	-3	60	-3	1

2.5 Boundary conditions

The boundary conditions applied in the simulation are the Dirichlet kind, which values are expressed in Table 3.

All the values were measured experimentally with exception of gravity.

2.6 Stability analysis

The convergence and numerical stability were obtained by monitoring the rate of change of the solution and the behavior of the dependent variables during the iterative process (Ite). Controlled variables were velocity (V), pressure (P), temperature (T), and turbulence quantities such as kinetic energy (degree of freedom ENKE) and kinetic energy dissipation rate (ENDS).

The convergence monitors (CM) are a normalized measure of the solutions rate of change from iteration to iteration. Considering ϕ a general variable, the convergence monitor could be defined as follows [25]:

$$CM=\frac{\sum_{i=1}^{n}\left|\phi_i^k-\phi_i^{k-1}\right|}{\sum_{i=1}^{n}\left|\phi_i^k\right|} \quad (14)$$

After initial fluctuations, convergence monitors decrease as the analysis approaches convergence.

Table 4 describes, for each case, the number of iterations (Ite), the computational time in hours (C(h)), and the residual for each variable (V_x, V_y, P, T, ENKE and ENDS).

The CPU time is relative high. This indicates that the mesh is probably too refined or the TDMA solver was not the best choice.

3. Results and discussion

3.1 Model validation

Fig. 4 shows a comparison between experimental

Table 4. Convergence of the adopted numerical procedure (CM values).

Case	Ite	C(h)	V_x	V_y	P	T	ENKE	ENDS
A	1.5×10^4	99	1×10^{-6}	1×10^{-6}	1×10^{-5}	1×10^{-7}	1×10^{-5}	1×10^{-5}
B	1.5×10^4	98	1×10^{-4}	1×10^{-4}	1×10^{-4}	1×10^{-6}	1×10^{-4}	1×10^{-3}
C	1.2×10^4	89	1×10^{-3}	1×10^{-3}	1×10^{-3}	1×10^{-5}	1×10^{-3}	1×10^{-2}

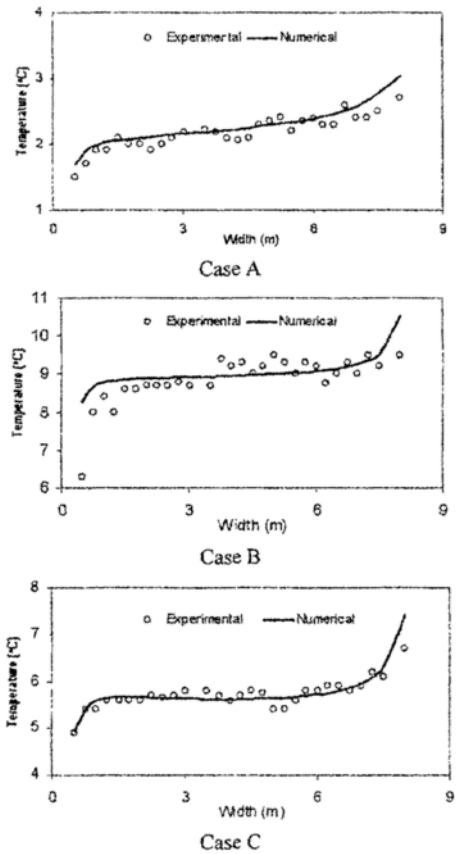

Fig. 4. Comparison between experimental and numerical results of temperature.

and numerical temperature values for the cases A, B and C.

The good agreement between the numerical and experimental temperature values validates the numerical procedure implemented in this work.

3.2 Temperature and velocity results

Figs. 5-9 show the temperature and velocity profiles for the five paths represented in Fig.1 and for the three cases studied in this work. The temperature and velocity patterns in the path AB are shown in Fig. 5. In the case A, the temperature is approximately constant and the airflow velocity is higher in the middle of the greenhouse. In the case B, an abrupt variation in the airflow velocity near the AHT is verified. This is due to natural convection, induced by the AHT. In the AHT coordinates the temperature has, as expected, a peak, which is also verified in case C. Between the cases B and C, the difference in the average temperature is about 3°C, which means that the natural ventilation causes significant energy losses. The airflow velocity is higher in case C, but only in a fraction of the path AB. This is due to the wind direction (right to left), which feeds the descending convection flow.

In the path CD, Fig. 6, the influence of the AHT and natural ventilation in the temperature is clearly shown - about 7°C in case B and about 3°C in case C. This influence is almost insignificant in the airflow

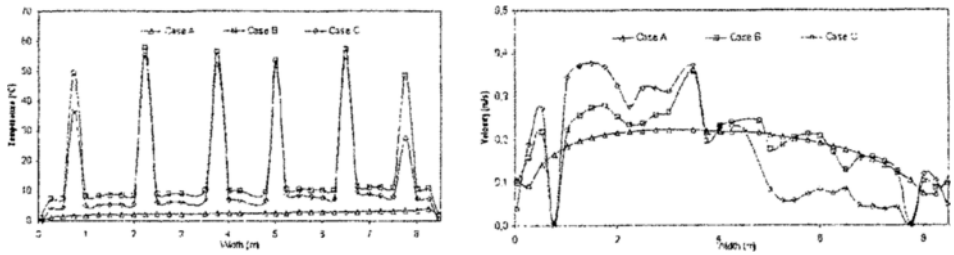

Fig. 5. Temperature and velocity profiles on path AB.

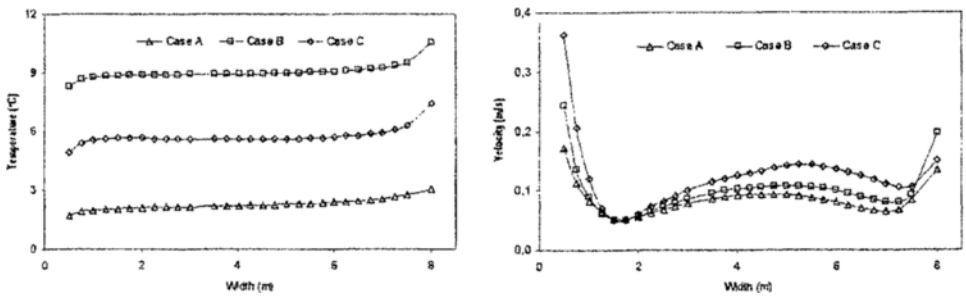

Fig. 6. Temperature and velocity profiles on path CD.

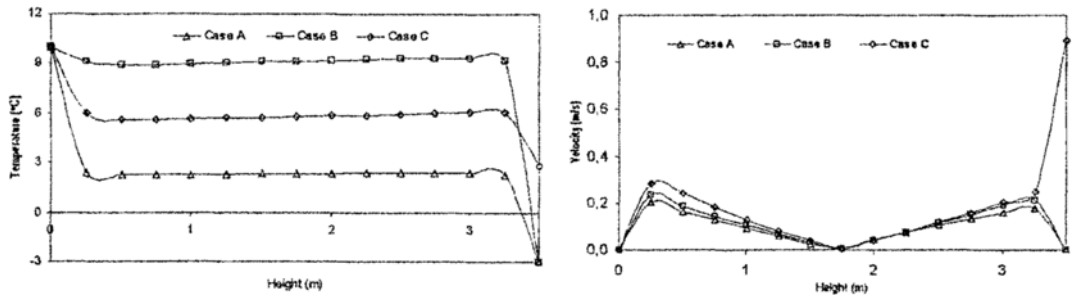

Fig. 7. Temperature and velocity profiles on path EF.

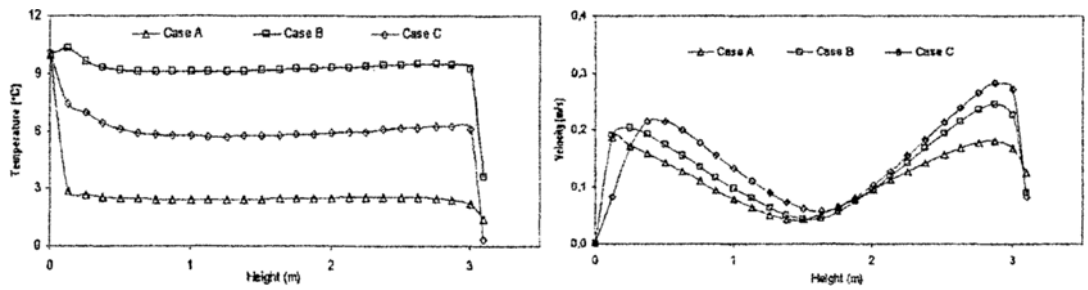

Fig. 8. Temperature and velocity profiles on path GH.

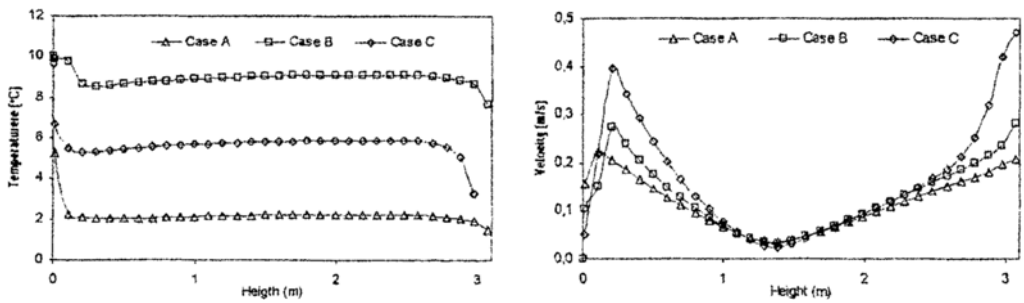

Fig. 9. Temperature and velocity profiles on path IJ.

velocity profile.

Fig. 7 shows (path EF) that the temperature values follow the same behavior of the path CD except in the top of the greenhouse, where the temperature reaches values below zero (point F – vent open). Notice that the airflow velocity increases strongly in this zone (case C) and becomes null in the middle of the path for all cases. This is because the center of the greenhouse is the nucleus of the main convective flow.

The temperature profile shown in Fig. 8 (path GH) is similar to those of Figs. 5 and 6. The airflow velocity profile is similar to the one of path EF, decreasing, however, in near the top of the greenhouse in case C. As far as temperature is concerned, a special note should be made for the thermal inversion that happens in all the vertical paths but is more visible in case B of Fig. 8. This behavior is explained by the position of the AHT system located at 0.125 m from the soil.

The average airflow velocity on path IJ, Fig. 9, is higher than path GH for all cases. This happens due to descendent airflow convection. However, on the path GH the airflow is contrary to gravity, which reduces the boundary effect.

4. Conclusion

The effects of heating tubes and natural ventilation on the indoor air temperature and velocity fields of Mediterranean greenhouses were numerical investigated by means of a CFD package in night conditions.

The incompressible Reynolds Averaged Navier-Stokes equations in conjunction with the RNG turbu-

lence model were used. This numerical approach avoids the use of most empirical heat transfer coefficients and provides adequate CPU time and residuals.

Three cases were studied, natural convective heating, artificial heating tubes, and artificial heating tubes and natural ventilation. Temperatures obtained numerically were compared with experimental data. The good agreement between numerical and experimental values allows the validation of the numerical procedure implemented in this work, and we may conclude that RNG turbulence model is suitable for simulating arch-shaped greenhouses microclimates.

As expected, the lowest average increase of the temperature is obtained in case A (2.2°C). Results show that the heating tubes (water flow at 60°C) allow increases of the indoor air temperature around 6.7°C. This fact is very important for the viability of many horticultural crops. If, away from the heating tubes, natural ventilation is introduced, the increase in temperature is 3.5°C. This is an important result, since it gives us an idea about the importance of the thermal losses in greenhouses.

The lowest turbulent regime is obtained in case A. When a heating system is introduced (case B), the turbulent regime increases slightly due to the natural convection. The highest turbulent regime is obtained in case C due to the combined effects of natural convection and ventilation. A phenomenon similar to the so-called 'side wall effect' was observed. Air velocity distribution along the greenhouse has a main circulation in the center of the greenhouse for all the studied cases.

The simulation of these processes using the *FLOTRAN* module of *ANSYS®* can be a good path to explore and some improvements can be done to this physical model: for instance, introducing night-time crop transpiration and making 3D simulations optimizing the size of the element mesh in order to reduce the computation time.

Nomenclature

Roman

A_c : Area of the greenhouse cover per unit ground area
a : Empirical constant
C : RNG turbulence model constants
c : Heat capacity
g : Gravity
k : Turbulent kinetic energy
K : Conductivity
P : Pressure
q : Heat flux
S : Solar radiation
t : Time
T : Temperature
U : Is the overall heat transfer coefficient
V : Velocity
$\dot{V}$: Air flow rate

Greek

β : Thermal expansion coefficient
ε : Rate of dissipation of turbulent kinetic energy
ϕ : General variable
η : Fraction of solar radiation converted in sensible heat
λ : Invariant
μ : Viscosity
Φ : Scalar
ρ : Density
σ : Stress

Subscripts

c : Conduction
d : Deep
e : Effective
g : Greenhouse
h : Virtual
lat : Latent
o : External
p : Pipe
r : Cover
s : Soil
sen : Sensible
sto : Stored
t : Time
v : Ventilation
rad : Solar radiation
x, y : Vector direction

References

[1] T. Boulard and A. Baille, A simple greenhouse climate control model incorporating effects of aeration and evaporative cooling, *Agric. For. Meteorol.* 65 (1993) 145-157.

[2] Sven Reichrath and Tom W. Davies, Using CFD to model the internal climate of greenhouses: past, present and future, *Agronomie* 22 (2002) 3-19.

[3] L. Okushima, S. Sase and M. A. Nara, Support system for natural ventilation design of greenhouses based on computational aerodynamics, *Acta Hortic.* 284 (1989) 129-136.

[4] S. Sase, T. Takakura and M. Nara, Wind tunnel testing on airflow and temperature distribution if a naturally ventilated greenhouse, *Acta Hortic.* 174 (1984) 329-336.

[5] A. Mistriotis, C. Arcidiacono, P. Picuno, G. P. A. Bot and G. Scarascia-Mugnozza, Computational analysis of ventilation in greenhouses at zero- and low-wind-speeds, *Agric. For. Meteorol.* 88 (1997) 121-135.

[6] A. Mistriotis, P. Picuno, G. P. A. Bot and G. Scarascia-Mugnozza, Computational study of the natural ventilation driven by buoyancy forces, Proceedings of the 3rd international workshop on mathematical and control applications in agriculture and horticulture, Pergamon Press (1997) 67-72.

[7] A. Mistriotis, G. P. A. Bot, P. Picuno and G. Scarascia-Mugnozza, Analysis of the efficiency of greenhouse ventilation using computational fluid dynamics, *Agric. For. Meteorol.* 85 (1997) 217-228.

[8] Y. S. Chen and S. W. Kim, Computation of turbulent flows using an extended k-ε turbulence closure model, NASA CR-179204 (1987).

[9] T. Boulard, J. F. Meneses, M. Mermier and G. Papadakis, The mechanisms involved in the natural ventilation of greenhouses, *Agric. For. Meteorol.* 79 (1996) 61-77.

[10] T. Boulard, R. Haxaire, M. A. Lamrani, J. C. Roy and A. Jaffrin, Characterization and modelling of the air fluxes induced by natural ventilation in a greenhouse, *J. Agric. Eng. Res.* 74 (1999) 135-144.

[11] R. Haxaire, J. C. Roy, T. Boulard, M. A. Lamrani and A. Jaffrin, Étude numérique et expérimentale de la ventilation par convection naturelle dans une serre, Actes Congr. Annu. SFT Marseille Elsevier Paris 5-7 May (1998) 64-69.

[12] R. Haxaire, J. C. Roy, T. Boulard, M. A. Lamrani and A. Jaffrin, Greenhouse natural ventilation by buoyancy forces, EPIC'98/11 Proceedings of the 2nd European Conference on Energy Performance and Indoor Climate in Buildings, École Nationale des Travaux Publics de l'État Lyon France (1998) 522-527.

[13] C. Müller, Modelling soil-biosphere interactions. CABI, Wallingford, UK. (2000).

[14] Z. S. Chalabi, B. J. Bailey and D. J. Wilkinson, A real-time optimal control algorithm for greenhouse heating, *Computers and Electronics in Agriculture* 15 (1996) 1-13.

[15] B. Bailey and W. Day, The use of models in greenhouse environmental control, *Acta Horticultura* 491 (1999) 93-99.

[16] R. Tap, L. Willigenburg and G. Straten, Experimental results of receding horizon optimal control of greenhouse climate, *Acta Horticultura* 406 (1996) 229-238.

[17] B. E. Launder and D. B, Spalding, The Numerical Computation of Turbulent Flows, *Computer Methods in Applied Mechanics and Engineering* 3 (1974) 269-289.

[18] J. J. Costa, L. A. Oliveira and D. Blay, Test of Several versions for the K-E type turbulence modelling of internal mixed convection flows, *International Journal of Heat and Mass Transfer* 42 (1999) 4391-4409.

[19] J. Kim and H. C. Choi, An immersed-boundary finite-volume method for simulation of heat transfer in complex geometries, *KSME Int. Journal* 18 (2004) 1026-1035.

[20] G. Kim, S. Kim and Y. Kim, Parallelized unstructured-grid finite volume method for modeling radiative heat transfer, *Journal of Mech. Science and Tech.* 19 (2005) 1006-1017.

[21] L. Monteiro, A. Rouboa and A. A. C. Monteiro, Heat transfer simulation in the mold with generalized curvilinear formulation, *Journal of Pressure Vessel Technology* 128(3) (2006) 462-466.

[22] V. Yakhot and S. A. Orszag, Renormalization group analysis of turbulence. Basic Theory, *J. Sci. Comput.* 1(1) (1986) 3-55.

[23] V. Yakhot and L. M. Smith, The Renormalization group, the eps-expansion and derivation of turbulence models, *J.Sci.Comput.* 7(1) (1992) 35-61.

[24] J. H. Ferziger and M. Perić, Computational Methods for Fluid Dynamics. 2nd edition, Springer Verlag, New York (1999).

[25] J. C. Tannehill, D. A. Anderson and R. H. Pletcher, *Computational Fluid Mechanics and Heat Transfer*, 2nd edition, Taylor & Francis Ltd. (1997).